Statistical Properties of an External-Cavity Semiconductor Laser: Experiment and Theory

Nianqiang Li, Wei Pan, A. Locquet, V. Chizhevsky, David Citrin

Statistical Properties of an External-Cavity Semiconductor Laser: Experiment and Theory

Journal:	*Journal of Selected Topics in Quantum Electronics*
Manuscript ID:	JSTQE-CON-SL2015-05682-2015
Manuscript Type:	Contributed
Date Submitted by the Author:	25-Jan-2015
Complete List of Authors:	Li, Nianqiang; Southwest Jiaotong University, Center for Information Photonics and Communications Wei, Pan; Southwest Jiaotong University, Center for Information Photonics and Communications Locquet, Alexandre; Georgia Institute of Technology, Department of Electrical and Computer Engineering Chizhevsky, V. N. ; B. I. Stepanov Institute of Physics, National Academy of Science of Belarus, 220072 Minsk, Belarus, Citrin, David; Georgia Institute of Technology, School of ECE;
Keyword:	Chaos, Semiconductor lasers, Statistics

Statistical Properties of an External-Cavity Semiconductor Laser: Experiment and Theory

Nianqiang Li, Wei Pan, Alexandre Locquet, *Member, IEEE,* V. N. Chizhevsky, and D. S. Citrin, *Senior Member, IEEE*

***Abstract*—We experimentally and numerically study the statistical properties of a semiconductor laser with time-delayed optical feedback. Our systematic analyses show that the statistical distribution of the raw intensity obtained from experiments is better fitted by a Laplacian distribution; both in experiments and simulations, the distribution pattern of the differential signal obtained from two independent intensities, as well as of that computed from its high-order finite differences, converges to a well-fitted Gaussian profile for high pump currents. This helps us understand the changes in statistical properties of the intensity with varying control parameters and achieve desired entropy sources for random number generators. Furthermore, in numerical simulations, we find the distribution of the differential signal undergoes a marked transition from a Gaussian to Laplacian profile as the feedback rate increases at low to moderate pump currents.**

***Index Terms*—Chaos, data fitting, semiconductor laser, statistical properties.**

I. Introduction

SEMICONDUCTOR lasers show a rich variety of dynamical behaviors when they are subject to external perturbations [1]–[4]. Time-delayed optical feedback is one of the simplest methods to generate a chaotic signal in semiconductor lasers [5], [6]. Laser chaos has attracted considerable interest for a range of applications and quite recently has been proposed as a promising candidate for high-speed physical random-number generators (RNGs) [7]–[14]. A crucial issue in RNGs is that the maximum rate of randomness extractible is closely related to the statistical properties of the entropy sources [8], [9], [11], [13]. In order to improve the bit rates of the generated random bit sequences, mirror symmetry of the statistical distribution of the chaotic output intensity is highly desired. That is, the statistical distribution of the intensity time series (sampled at some specified rate) is desired to be symmetrical with respect to the mean value (equal to the median for a symmetric distribution). Unfortunately, the distribution of the raw time series (RTS) obtained from the light intensity generated by semiconductor lasers with time-delayed optical feedback [external-cavity semiconductor lasers (ECLs)] is never ideally symmetric, and in many cases the departure from symmetry is quite strong.

Much research has been devoted to understanding the intensity statistics of ECLs operating in the low-frequency-fluctuations (LFF) regime [15]–[17], where the average laser intensity shows repetitive dropouts and gradually recovers on a very long timescale (typically tens of external-cavity round-trip times). This dropout behavior skews the intensity distribution toward zero intensity, leading to an extremely asymmetric probability-density function (PDF) of the laser intensity. Previous experimental studies have shown that, for truly single-mode emission, PDFs peak just above the spontaneous-emission level and decrease monotonically with increasing intensity [16], [17]. These investigations have also shown that numerical simulations of the conventional single-mode Lang-Kobayashi (LK) model [16], [17] are sufficient to reproduce the main features of the experimental PDFs. Studies of the intensity statistics of ECLs in the coherence-collapse (CC) regime are scarce [18], [19], in contrast to those of LFF dynamics. CC means the laser linewidth broadens drastically from a few MHz to typically 10-25 GHz, which is a particular interesting feature of an ECL [20]. During the past few years a few experimental works aiming at ultrafast RNG using chaotic lasers in the CC regime have reported that the distribution of the ac component of the intensity in some cases appears roughly Gaussian, but slightly skewed [8], [13], [14]. Moreover, it has been numerically demonstrated that the intensity PDF converges to a unique distribution for chaotic lasers with specified parameters [21], and the distribution does not necessarily have Gaussian statistics due to the physical constraints of the working points and laser parameters [22]. In the above cited reports, the ECL operates in either the LFF or CC regime for a fixed optical feedback level. However, it is still unclear whether the statistical properties of chaotic ECLs will change when varying the control parameters, i.e., injection current J and feedback rate. For example, in a certain time-delayed chaotic system, the PDFs for the outputs evolved from non-Gaussian to Gaussian-like profile with increasing feedback rate [23] or J [18].

On the other hand, based on the preceding literature review,

Manuscript received January 26, 2015; revised 2015. This work was supported by the National Natural Science Foundation of China under Grant 61274042, in part by the Conseil Regional of Lorraine under Grant GT-CNRS2958, in part by the National Science Foundation under Grant ECCS-0925713, and in part by the Funds for the Excellent Ph.D. Dissertation of the Southwest Jiaotong University (2011).

N. Li and W. Pan are with the Center for Information Photonics and Communications, Southwest Jiaotong University, Chengdu, 610031 China (email: wan_103301@163.com; weipan80@sina.com).

A. Locquet and D. S. Citrin are with the Department of Electrical and Computer Engineering, Georgia Institute of Technology, Atlanta, GA 30332-0250 USA, and also with the UMI 2958 Georgia Tech-CNRS, Georgia Tech Lorraine, 2 rue Marconi, Metz 57070, France (e-mail: alexandre@gatech.edu; david.citrin@ece.gatech.edu).

V. N. Chizhevsky is with the B. I. Stepanov Institute of Physics, National Academy of Science of Belarus, 220072 Minsk, Belarus (email: vnc@dragon.bas-net.by).

Color versions of one or more of the figures in this paper are available online at http://ieeexplore.ieee.org.

Digital Object Identifier

it would appear problematic to obtain a symmetric intensity PDF without introducing any post-treatment of the chaotic signals generated by ECLs. Fortunately, several efficient general approaches for transforming the raw asymmetric PDF into a highly symmetric one have been developed [8], [24]–[27]. Among them, differential comparison is commonly employed to symmetrize the intensity statistics [24], [25]. To be precise, let X1, X2 (RTS) be independent, identically distributed (i.i.d.) random variables, then the difference Y=X1−X2 has a symmetric PDF [26]. [Note that the differential signal Y is termed as the post-processed time series (PTS) throughout this paper.]. So far however, to our knowledge, there are no detailed studies of this procedure applied to ECLs that output fully developed chaos, nor comparisons of experimental and numerical results over a wide range of tunable system parameters. The comparison between theoretical and experimental results is particularly important for understanding and tailoring the intensity statistics of the chaotic laser sources, so as to develop chaotic laser-based RNGs. Furthermore, it is no surprise that enhancement of the symmetry of the PDF can lead to substantial increase in the rate at which the random bits can be generated when multi-bit extraction schemes are adopted [9], [26], [27].

In this paper, we investigate experimentally and numerically the statistical properties of the intensity fluctuations of ECLs operating in the chaotic regime, the external cavity supplying the (optical) time-delayed feedback. To demonstrate the robustness and the generality of the observations, two independent experiments are performed with two different single-mode distributed feedback (DFB) lasers subject to free space-optic feedback provided by a mirror and to fiber-optic feedback, respectively. Numerical simulations of the single-mode LK model are used to confirm the observations. Throughout the study, two standard statistics, i.e., Gaussian and Laplacian, are utilized to fit the PDFs of the experimental and theoretical intensity time series generated by the chaotic ECLs, except for theoretical RTS. We show that simulations of the LK model are in good qualitative agreement with experiments. Specifically, we identify that the PDF of the theoretical PTS undergoes a notable transition from a Gaussian to a Laplacian profile as the feedback level increases at low to moderate J, and reveal changes in the underlying dynamics based on the time series and its phase-space trajectory.

II. Experiment

We perform two independent experiments, using different single-mode DFB lasers emitting at 1550 nm, under different feedback conditions, and two data-acquisition systems. One employs freespace components to provide the external cavity. The other uses an external cavity consisting of fiber-optic components. The former is termed as experiment 1 and the latter as experiment 2.

A. Experiment 1: Freespace

The setup for experiment 1 is depicted in Fig. 1(a). It consists of an intrinsically single-longitudinal-mode MQW InGaAsP DFB laser, exhibiting maximum cw power of 15 mW. The free-running laser threshold current $J_{th} \sim 9.27$ mA. The laser diode (LD) receives delayed feedback from a mirror (M), via a beam splitter (BS). The BS divides the light intensity equally to two freespace paths: one is used for feedback into the LD and the other for detecting the optical intensity. The position of M determines the feedback time delay for the LD and is set to 65 cm, corresponding to external-cavity round-trip time of ∼4.3 ns. With the help of a motorized rotation stage, the angle of a quarter-wave plate (QWP) is controlled in small steps. The maximum feedback (experimental feedback rate $\eta = 1.0$) is reached when the QWP is such that the polarization is not subject to any rotation. In this experiment, ∼20 % of the optical power is fed back onto the collimating lens for $\eta = 1.0$. J is held well above J_{th} throughout this study. A fast PD (New focus 1544-B Multimode) with 12 GHz bandwidth is used to convert the optical intensity fluctuations into an electrical signal. A 12 GHz bandwidth, 40 GS/s real-time OSC (Agilent DSO80804B) is employed to capture the resulting time series for analysis.

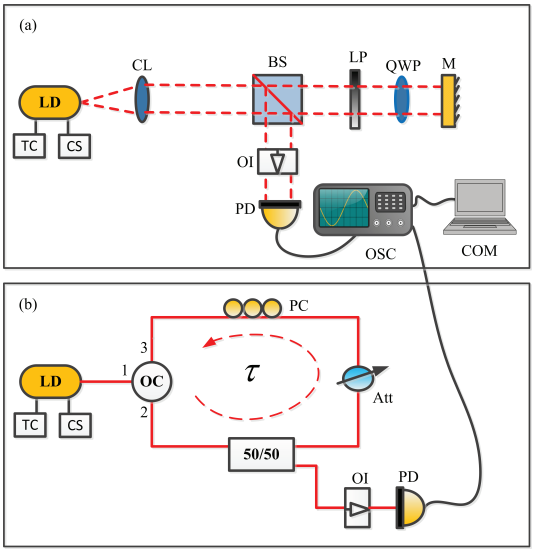

Fig. 1. Schematic of the experiment: (a) freespace (experiment 1), (b) fiber-based (experiment 2). LD stands for laser diode, CL for collimator lens, BS for beam splitter, LP for linear polarizer, QWP for quarter-wave plate, M for mirror, OI for optical isolator, PD for photodiode, OSC for oscilloscope, COM for personal computer, PC for polarization controller, OC for optical circulator, Att for optical attenuator, TC for temperature controller and CS for current supply.

B. Experiment 2: Fiber-based

The setup for experiment 2 is depicted in Fig. 1(b). The LD used in this experiments is another intrinsically single-longitudinal-mode DFB laser that is connected by fiber pigtails and has $J_{th} \sim 10$ mA. The output light is fed back into the laser facet after it passes through a fiber ring cavity that consists of an optical circulator (OC), a variable optical attenuator (Att), a polarization controller, and a 50:50 fiber coupler. The feedback delay is estimated to be ∼ 79 ns and originates from the fiber-optic components used in the experiment. The feedback power is controlled by the Att. The

experimental feedback rate is estimated as the ratio of the feedback power and the output power of the stand-alone LD. The feedback power is measured just before the feedback light enters the LD and is larger than the actual feedback level because the coupling efficiency of which we are uncertain is not included. Likewise, the maximum feedback power attained in this experiment is $\sim 14\,\%$ of the solitary laser output power, corresponding to experimental feedback rate $\eta = 1.0$. The ECL output is captured by high-speed PD (HP 11982A) with a bandwidth of 10 GHz. The resulting electrical signal is then sent to a digital OSC (LeCroy WaveMaster 813 zi, 13 GHz) and recorded at the sampling rate of 40 GS/s.

III. Numerical Model

A well verified model to describe single-mode ECLs is the LK equations for the complex slowly varying amplitude of the electric field $E(t)$ and carrier number inside the cavity $N(t)$ [6], [28], [29]. These equations are given by

$$\dot{E}(t) = \frac{(1+i\alpha)}{2}\left[G(t) - \frac{1}{\tau_p}\right]E(t) + \gamma E(t-\tau)\,e^{-i\Psi}, \quad (1)$$

$$\dot{N}(t) = \frac{J}{e} - \frac{N(t)}{\tau_N} - G(t)\,|E(t)|^2, \quad (2)$$

where $G(t) = g(N(t) - N_0)/(1 + s\,|E(t)|^2)$ is the optical gain (with g being the differential gain coefficient and s the saturation coefficient), N_0 the carrier density at transparency, α the linewidth-enhancement factor, Ψ optical feedback phase, τ_p the photon lifetime, τ_N the carrier lifetime, γ the theoretical feedback rate, τ the feedback time delay, and $J = qJ_{th}$ the pump current(with q being the pump factor). We consider the following values for the above parameters: $\alpha = 5$, $\tau_p = 2$ ps, $\tau_N = 2$ ns, $g = 1.5 \times 10^{-8}$ ps^{-1}, $N_0 = 1.5 \times 10^8$, $\Psi = 0$, $\tau = 1$ ns. With these parameter values, the threshold current J_{th} of the solitary laser is 14.7 mA. The two control parameters γ and q are varied in our simulations. We omit spontaneous emission noise not only for simplicity but also because we find numerically that the inclusion of the noise term does not significantly modify the dynamics, especially for the relatively large J considered here.

Eqs. (1) and (2) are integrated with a fourth-order Runge-Kutta algorithm with a time step of 1 ps, and the corresponding numerical results will be presented in Sec. IV. Unless explicitly stated, the sampling rate is set to 40 GS/s, corresponding to the experimental condition.

IV. Results

In this section, we present the experimental and numerical results of the intensity statistics of the RTS and PTS generated by a single-mode ECL. We compare the experimental results obtained from both experiments to those obtained from numerical simulations of the LK model. Note that all PDFs are derived from 3.9×10^4 data points for both experiments and simulations, unless otherwise specified.

Figure 2 (a) shows an example of the temporal waveform observed in experiment 1 and (b) presents the corresponding autocorrelation, with $J = 1.4J_{th}$ and $\eta = 0.41$. The first peak

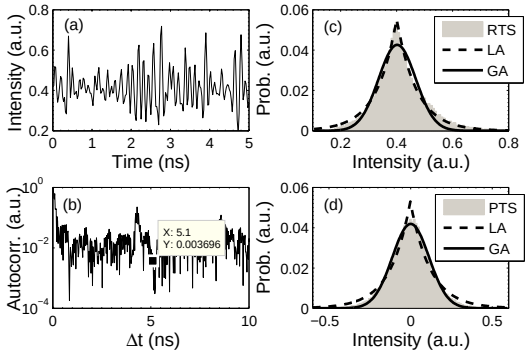

Fig. 2. Experiment 1: (a) Intensity time series, (b) autocorrelation, and PDFs of (c) RTS and (d) PTS. The dashed and solid lines are fitted Laplacian and Gaussian curves. LA stands for Laplacian, and GA for Gaussian.

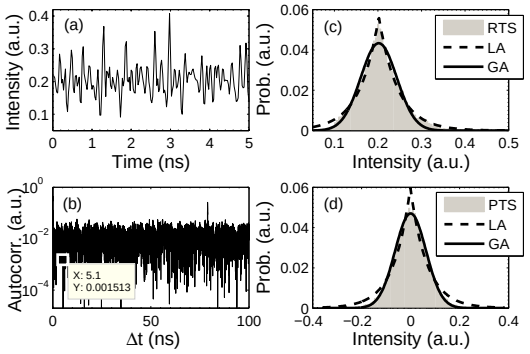

Fig. 3. Same as in Fig. 2, but for Experiment 2.

of the autocorrelation appears at ∼4.3 ns, corresponding to the round-trip time of the external cavity [30], [31].

Figures 2(c) and (d) show the PDFs of the RTS and PTS. Here, the PTS (Y) is obtained by subtracting the RTS (X1) of the laser from the same output (X2) numerically delayed by 5.1 ns. Note that in our experiment only one PD was used so we numerically shifted the chaotic output, but the difference between intensity time series can also be realized physically by having two PDs with an electrical time delay as would be desirable for practical RNGs. The two temporal waveforms are effectively independent since the correlation is only $\sim 3.696 \times 10^{-3}$ at 5.1 ns (which is intentionally not a multiple of the optical time delay 4.3 ns), as shown in Fig. 2(b). Therefore, a symmetric distribution of the PTS (Y=X1−X2) can be expected. A casual perusal of the two histograms shows that the PDF of the PTS is much more symmetric, which is quantitatively confirmed by calculating the skewness $S = \mu_3/\sigma^3$ [26], where μ_3 and σ the third central moment and the standard deviation, respectively, i.e., $|S| \approx 1.4 \times 10^{-4}$ for the PTS which is near the ideally symmetric distribution.

A Gaussian profile is desirable for RNG [18]. Despite the fact that the PDF of the ECL is not Gaussian, it is still of interest to explore how the actual PDFs deviate from the desired statistics. We note that some previous reports have shown that the PDF of unprocessed experimental time series

appears roughly Gaussian or Laplacian [8], [11], [13], [14], [18], [19]. Therefore, to gain more insight into the statistics of the chaotic ECLs, Gaussian and Laplacian distributions are utilized to fit the calculated PDFs. Fig. 2 (c) shows the histogram of the RTS is better fitted by a Laplacian. In contrast to the statistics of the RTS, it is interesting to observe that the PDF of the PTS in this experiment is highly Gaussian [Fig. 2 (d)], whereas the best Laplacian fit is quite poor. This could be expected, since the distribution of the RTS already has certain features of Gaussian statistics and the standard deviation is increased by performing the differential comparison. The larger the standard deviation, the flatter and broader the PDF we can obtain. Consequently, the obtained PDF more closely resembles a Gaussian. In fact, the density of the sum of two independent real-valued random variables equals the convolution of the density functions of the original variables. Therefore, X1−X2 can be regarded as the sum of independent random variables X1 and −X2. The convolution of these, then, is the autocorrelation of the distribution of the RTS. Upon successive convolutions, it is not surprising that the resulting distribution tends to a Gaussian, as stated in the central limit theorem.

The above procedures are applied to the data obtained from experiment 2 and similar phenomenon can be observed. An example of the results for experiment 2 is displayed in Fig. 3, where $J = 1.4J_{th}$ and $\eta = 0.2$. As can be seen, the first peak of the autocorrelation appears at $\sim$ 79 ns, corresponding to the round-trip time of the external cavity. Indeed, we confirm that the PDF of the RTS is better fitted by a Laplacian, while that of the PTS is closer to a Gaussian.

The Gaussian and Laplacian fits are further quantified by an R^2 test [18]. To be precise, R^2 is the square of the correlation between the observed data and the expected or fitted values. This metric can take any value between 0 and 1, with a value closer to 1 indicating a better fit.

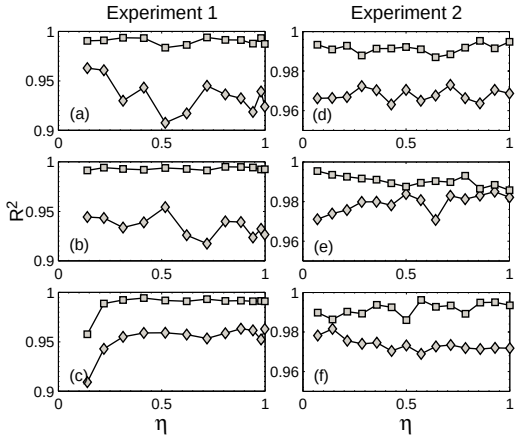

Fig. 4. R^2 comparison as a function of η for the RTS in both experiments. (a, d) Results for $J = 1.4J_{th}$; (b, e) for $J = 1.7J_{th}$; and (c, f) for $J = 2.4J_{th}$. (a-c) Experiment 1 and (d-f) experiment 2. Open squares correspond to Laplacian; open diamonds to Gaussian.

Figure 4 shows R^2 for the RTS as a function of η in both experiments. Three pump values $J \gg J_{th}$ are chosen: $J = 1.4J_{th}$ (a, d), $J = 1.7J_{th}$ (b, e), and $J = 2.4J_{th}$ (c, f). The feedback rate η is such that the ECL operates in the chaotic regime. It is apparent that the Laplacian fit is substantially better for all operating J and η considered in the experiments, when compared with the Gaussian fit. This indicates that the PDFs of chaotic optical intensity of ECLs, subject to optical feedback either provided by freespace or fiber-based optical components, more closely resembles a Laplacian. It is worth emphasizing that, for the case of the RTS, numerical simulations of the LK model do not reproduce these behaviors due to several uncertain physical constraints, such as the bandwidth of the experimental detection system, the laser parameters and limitations intrinsic to the LK model. Although the above constraints were taken fully into account, we did not obtain a Laplacian shape for the PDF of the RTS obtained from the LK model as described in our recent paper [19]; hence these numerical PDFs are not fitted and compared to the experiments.

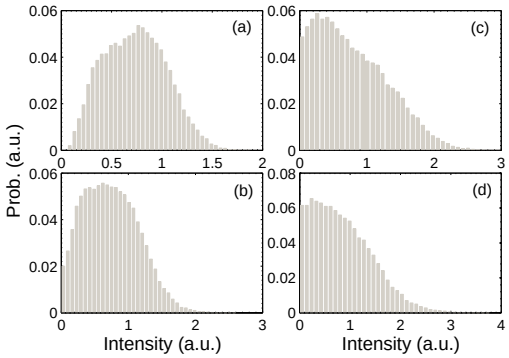

Fig. 5. PDFs of RTS in LK model for four γ, when $J = 1.4J_{th}$. (a) $\gamma = 10$ ns^{-1}; (b) $\gamma = 15$ ns^{-1}; (c) $\gamma = 30$ ns^{-1}; and (d) $\gamma = 50$ ns^{-1}.

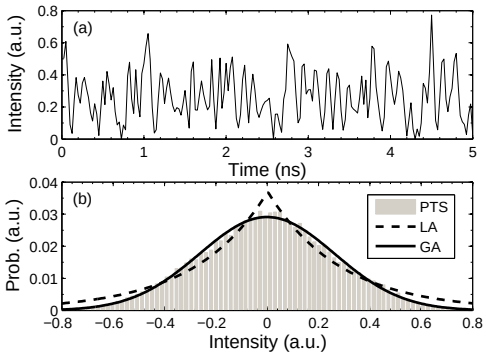

Fig. 6. (a) Intensity time series generated by the LK model when $J = 1.4J_{th}$ and $\gamma = 30$ ns^{-1}, and (b) PDF of PTS. The dashed and solid lines are the fitted Laplacian and Gaussian. LA stands for Laplacian, and GA for Gaussian.

In Fig. 5, we show an example of the PDFs of the RTS obtained from the LK model for four values of γ, when $J = 1.4J_{th}$. This figure summarizes the transition from Gaussian-shaped statistics of the RTS when γ is small to long-tailed statistics with increasing probability for high-frequency, low-amplitude components when γ is sufficiently larger.

In the following we choose to make detailed comparisons between experiments and simulations based on the PTS. In the

same way as we did for the experiments, we now examine the PDFs of the PTS obtained from the LK model. Here the PTS is obtained by taking the difference between the RTS and itself offset (numerically) by a time delay of 3.65 ns, consistent with the process in our experiments. The numerical time delay is chosen to ensure that the chaotic time series and its delayed replica are effectively independent. Fig. 6 (a) shows the typical RTS obtained from the LK model and (b) is the corresponding PDF of the PTS. We find that, in this numerical case, the PDF of the PTS is also better fitted by a Gaussian, which is in very good agreement with the experimental results presented in Figs. 2 and 3.

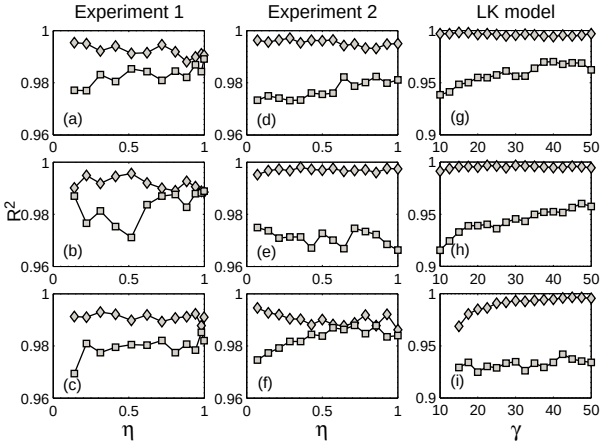

Fig. 7. R^2 comparison as a function of η (γ) for the PTS in both experiments as well as in the LK model. (a, d, g) $J = 1.4J_{th}$; (b, e, h) $J = 1.7J_{th}$; and (c, f, i) $J = 2.4J_{th}$. (a-c) Experiment 1; (d-f) experiment 2: and (g-i) LK. Open squares correspond to Laplacian; open diamonds to Gaussian.

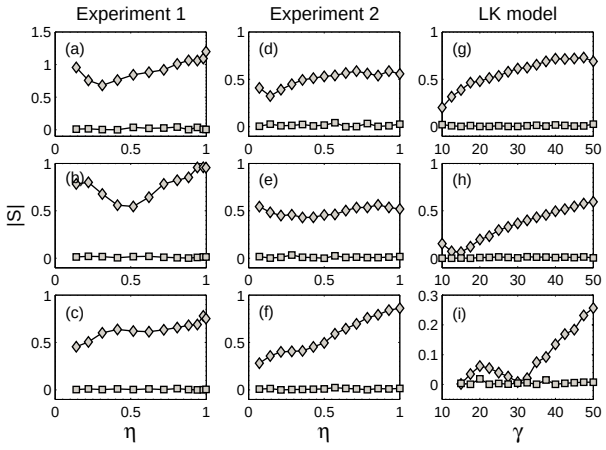

Fig. 8. $|S|$ comparison as a function of η (γ) for the RTS and PTS in both experiments as well as in the LK model. (a, d, g) $J = 1.4J_{th}$; (b, e, h) $J = 1.7J_{th}$; and (c, f, i) $J = 2.4J_{th}$. (a-c) Experiment 1; (d-f) experiment 2: and (g-i) LK. Open squares correspond to $|S|$ for the RTS; open diamonds to $|S|$ for the PTS.

We now evaluate R^2 for the PTS as a function of η (γ) in both experiments and LK model, as shown in Fig. 7. Similarly to what we obtained for the RTS case, three values of $J \gg J_{th}$ are considered: $J = 1.4J_{th}$ (a, d, g), $J = 1.7J_{th}$ (b, e, h), and $J = 2.4J_{th}$ (c, f, i). In all cases, the features of these experimental data are in good agreement with the numerical findings: the statistics of the PTS are more Gaussian than Laplacian for the considered J and η (γ). A careful analysis of Fig. 7 allows us, however, to notice quantitative discrepancies among numerics and both experiments for the absolute value of R^2, possibly related to the influence of noise, to the uncertain calibration of experimental parameters, as well as to the limitations intrinsic to the model.

Comparison between Figs. 4 and 7 shows, over a wide range of control parameters, the PDFs computed from the RTS are better characterized by Laplacian statistics, whereas those from the PTS are better fitted by Gaussian statistics. The central limit theorem helps to understand the convergence toward a Gaussian due to the post-treatment. In addition, we turn to quantify the great improvement in the degree of symmetry in the distribution. To this end, the statistical properties of the RTS and PTS are evaluated in terms of another metric, i.e., the skewness of the PDF S. The results are shown in Fig. 8. As expected, we observe that $|S|$ of the PTS in both experiments and LK model tends to zero, the RTS always exhibits pronounced asymmetry depending on J and η (γ). In addition, it is also shown in simulations that $|S|$ computed from the RTS is small for small to moderate γ [e.g., see Figs. 8 (h) and (i)]. This is because gain saturation in the LK model with small to moderate γ can suppress strong pulsations of laser intensity which are seen for large γ. In this case, the resulting PDF looks more symmetric and the peak value is located at around the average intensity [e.g., see Fig. 5 (a)], resulting in small values of S.

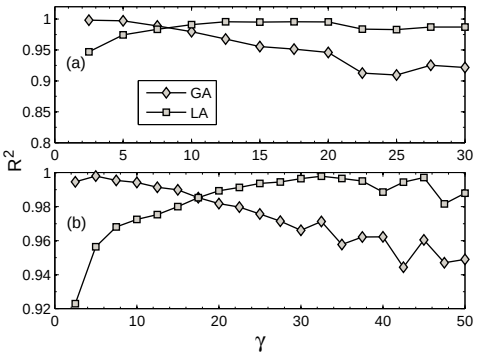

Fig. 9. R^2 comparison as a function of γ for the PTS in LK model. (a) $J = 1.05J_{th}$ and (b) $J = 1.1J_{th}$. Open squares correspond to Laplacian; open diamonds to Gaussian. LA stands for Laplacian, and GA for Gaussian.

In Figs. 7 and 8, there is a good qualitative agreement between experiments and simulations. The filtering effect due to the PD and OSC bandwidth is not taken into account. More specifically, the theoretical time traces are not filtered by using a low-pass filter of narrow bandwidth, as we did in [19]. However, we have confirmed that it has no significant impact on the results obtained here because of the presence of post-processing.

In addition to these consistent experimental and numerical results, Fig. 9 studies lower values of the current and shows a transition from Gaussian statistics of the PTS in the simulations when γ is small to moderate to Laplacian statistics

when γ is larger, for low values of J [e.g., $J = 1.05J_{th}$ in Fig. 9 (a) and $J = 1.1J_{th}$ in Fig. 9 (b)]. That is, as provided by the curves of R^2, the Gaussian fit is better for small values of γ; instead, when γ is increased above a critical value, the Laplacian fit is better. Moreover, comparison between Figs. 9 (a) and (b) shows that the critical value of γ related to the transition increases with increasing J.

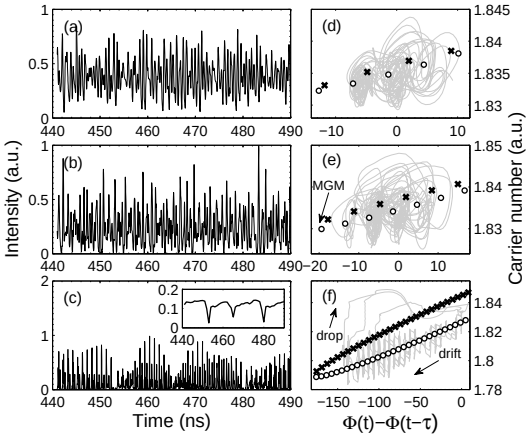

Fig. 10. (a-c) Intensity time series and (d-f) the projection on the plane of carrier number and phase difference $\Phi(t) - \Phi(t-\tau)$ for $J = 1.05J_{th}$ with (a, d) $\gamma = 2.5$ ns^{-1}, (b, e) $\gamma = 5$ ns^{-1}, and (e, f) $\gamma = 35$ ns^{-1}. MGM: maximum gain mode. Crosses mark the unstable fixed points (antimodes), circles indicate the stable fixed points (ECMs). The inset shows intensity at 1 GHz obtained from numerical simulations.

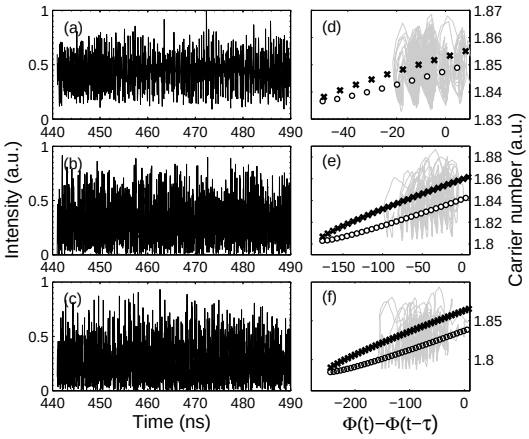

Fig. 11. (a-c) Intensity time series and (d-f) the projection on the plane of carrier number and phase difference $\Phi(t) - \Phi(t-\tau)$ for $J = 1.5J_{th}$ with (a, d) $\gamma = 10$ ns^{-1}, (b, e) $\gamma = 35$ ns^{-1}, and (e, f) $\gamma = 50$ ns^{-1}.

To gain more insight into the above transition, we show in Figs. 10 and 11 the intensity time series (RTS) corresponding to qualitatively different PDFs as well as the trajectory projected on the plane of carrier number versus phase difference $\Phi(t) - \Phi(t-\tau)$ [32]. In this plane, the two types of stationary solutions of the LK equations, namely the external-cavity modes (ECMs) and unstable antimodes, which are saddle points, are known to lie on an ellipse.

We find that the above transition is associated with the predominant dynamical behaviors obtained from the LK model. It is clear that, as γ is increased, the optical intensity tends to pulsate. This means the intensity time series has a more spiky appearance and shows more small-amplitude fluctuations for larger γ, which is evident in Figs. 10 (a)-(c). Thus, at moderately strong γ, higher sporadic peaks combined with the large amount of low-intensity components constitute a single-sided PDF with a long tail on high intensities.

We would like to stress that the underlying dynamics can be related to the phase-space trajectory that moves amongst the ECMs and antimodes. When J is fixed, increasing γ, several ECMs may become unstable and participate in the dynamics [32]. As an example, one can clearly see that more neighboring attractors begin to join the merged global attractor for larger γ based on the comparison between Figs. 10 (d) and (e) for $J = 1.05J_{th}$, as well as the results in Figs. 11 (d)-(f) for $J = 1.5J_{th}$. This results in the trajectory reaching regions of higher intensity [33], as well as more frequently visiting the low-intensity region of phase space, which in turn determines the PDF. We point out that for a small J ($J = 1.05J_{th}$), when γ is increased to a moderate level the system operates in the LFF regime [see Fig. 10 (c)], where the dynamics are characterized by chaotic itinerancy with a drift towards the MGM. In this regime, the intensity time series can be characterized by randomly occurring sudden drops and subsequent stepwise buildup [see the inset in Fig. 10 (c), in which we filtered the intensity with a 1-GHz Butterworth low-pass filter]. Moreover, pronounced pulsating dynamics occur in the LFF regime as can be seen in Fig. 10 (c). More generally, as long as the ECL does not produce pronounced pulsating dynamics, the PDF has a maximum at well above zero level. In this case, a Gaussian for the PTS is expected. On the other hand, when pulsating dynamics occur, in between two pulses the intensity of the ECL is nearly zero. These small-amplitude components of the intensity contribute to the appearance of a roughly exponential distribution for the RTS (not shown), where the probability for low intensity is extremely high. As a result, the transition to Laplacian statistics for the PTS is expected, since the difference between two i.i.d. exponential random variables is governed by a Laplacian distribution which can indeed be identified based on larger values of R^2 for Laplacian statistics in Fig. 9.

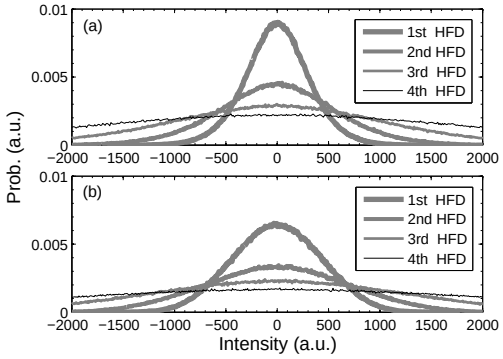

Fig. 12. PDFs of 1st-4th HFD of the PTS computed from (a) experimental and (b) numerical data. HFD represents high-order finite differences. Sampling rate: 20 GHz; the used data points: 10^6.

Finally, we consider another post-treatment of the intensity time series by computing consecutively the difference sequence between two neighboring samples in the PTS to further achieve consistent results between experiments and simulations. This post-processing method, called high-order finite differences (HFD) [26], [27], allows one to transform asymptotically any nonsymmetrical distribution into a perfectly symmetrical one. Fig. 12 displays the evolution of the PTS statistics when the HFD processing is iterated several times: (a) corresponds to experiment and (b) to simulation. Again, the trends in experiment are in good agreement with the theoretical expectations based on the LK model; by increasing the number of difference operations performed, the PDF becomes more symmetric, more closely resembling a Gaussian distribution; the changes in its width and height also exhibit similar behaviors. It should be noted, however, that we have considered a lower sample rate (20 GHz) in our experiment and simulation to achieve the consistency shown in Fig. 12. The detailed analysis of this issue is an objective for future studies.

V. Conclusion

In summary, we have studied experimentally and numerically the statistical properties of a chaotic ECL when η (γ) is varied, for several J. Two types of experimental setups based on two different DFB lasers were considered: in one, a DFB laser is subject to freespace feedback provided by a mirror and, in the other, another DFB laser is subject to feedback provided by an optical fiber loop. We have shown that, in both experiments, the PDFs of the RTS generated by the ECLs operating in a CC regime are better characterized by Laplacian statistics. For the case of the PTS, the PDFs are better fitted by Gaussian statistics in both experiments as well as in the LK model when $J \gg J_{th}$. When compared with the PDFs computed from the RTS, the PDFs computed from the PTS always show significantly higher degree of symmetry, as characterized by the skewness coefficient S. Additionally, numerical simulations of the LK model show that, at low J, a pronounced transition from Gaussian to Laplacian is identified for the PDFs computed from the PTS as γ is increased above a critical value. This, however, is explained based on the intensity time series as well as the trajectories in phase space. Finally, the widely used post-treatment method called HFD has been performed for the PTS and consistency between the experiments and simulations has been achieved. These findings also confirm that the post-processing can substantially improve the dynamical properties at the expense of additional numerical processing, especially when HFD is used. We expect this deeper understanding of the statistical properties of the ECLs may have broad applicability and lead to improvements of chaos-based RNGs.

References

[1] G. H. M. Van Tartwijk and D. Lenstra, "Semiconductor lasers with optical injection and feedback," *Quantum Semiclass. Opt.,* vol. 7, pp. 87-143, 1995.

[2] M. C. Soriano, J. Garcia-Ojalvo, C. R. Mirasso and I. Fischer, "Complex photonics: Dynamics and applications of delay-coupled semiconductor lasers," *Rev. Mod. Phys.,* vol. 85, pp. 421-470, 2013.

[3] J. Ohtsubo, *Semiconductor Lasers: Stability, Instability and Chaos.* New York, USA: Springer-Verlag, 2006.

[4] V. N. Chizhevsky, "Enhancement of response of a bistable VCSEL to modulated orthogonal optical feedback by vibrational resonance," *Opt. Lett.,* vol. 37, pp. 4386-4388, 2012.

[5] A. Locquet, C. Masoller, and C. R. Mirasso, "Synchronization regimes of optical-feedback-induced chaos in unidirectionally coupled semiconductor lasers," *Phys. Rev. E,* vol. 65, p. 056205, 2002.

[6] W. Zhang, W. Pan, B. Luo, X. Li, X. Zou, and M. Wang, "Theoretical study on polarization dynamics of VCSELs with negative optoelectronic feedback," *Appl. Opt.,* vol. 46, pp. 7262-7266, 2007.

[7] A. Uchida, K. Amano, M. Inoue, K. Hirano, S. Naito, H. Someya, I. Oowada, T. Kurashige, M. Shiki, S. Yoshimori, K. Yoshimura, and P. Davis, "Fast physical random bit generation with chaotic semiconductor lasers," *Nat. Photonics,* vol. 2, pp. 728-732, 2008.

[8] I. Reidler, Y. Aviad, M. Rosenbluh, and I. Kanter, "Ultrahigh-speed random number generation based on a chaotic semiconductor laser," *Phys. Rev. Lett.,* vol. 103, p. 024102, 2009.

[9] A. Argyris, S. Deligiannidis, E. Pikasis, A. Bogris, and D. Syvridis, "Implementation of 140Gb/s true random bit generator based on a chaotic photonic integrated circuit," *Opt. Express,* vol. 18, pp. 18763-18768, 2010.

[10] Y. Wang, P. Li, and J. Zhang, "Fast random bit generation in optical domain with ultrawide bandwidth chaotic laser," *IEEE Photon. Technol. Lett.,* vol. 22, pp. 1680-1682, 2010.

[11] N. Oliver, M. C. Soriano, D. W. Sukow, and I. Fischer, "Dynamics of a semiconductor laser with polarization-rotated feedback and its utilization for random bit generation," *Opt. Lett.,* vol. 36, pp. 4632-4634, 2011.

[12] R. M. Nguimdo, G. Verschaffelt, J. Danckaert, X. Leijten, J. Bolk, and G. V. Der Sande,"Fast random bits generation based on a single chaotic semiconductor ring laser," *Opt. Express,* vol. 20, pp. 28603-28613, 2012.

[13] T. Yamazaki and A. Uchida, "Performance of random number generators using noise-based super-luminescent diode and chaos-based semiconductor lasers," *IEEE J. Sel. Top. Quantum Electron.,* vol. 19, p. 0600309, 2013.

[14] X. Li and Sze-Chun Chan, "40 Gps random bit generation by oversampling chaos from an injected semiconductor laser," *Proc. of SPIE 8552,* p. 85520K, 2012.

[15] G. Huyet, S. Hegarty, M. Giudici, B. DE Bruyn and J. G. Mcinerney, "Statistical properties of the dynamics of semiconductor lasers with optical feedback," *Europhys. Lett.,* vol. 40, pp. 619-624, 1997.

[16] D. W. Sukow, T. Heil, I. Fischer, A. Gavrielides, A. Hohl-AbiChedia, and W. Elsäßer, "Picosecond intensity statistics of semiconductor lasers operating in the low-frequency fluctuation regime," *Phys. Rev. A,* vol. 60, pp. 667-673, 1999.

[17] G. Huyet, J. K. White, A. J. Kent, S. P. Hegarty, J. V. Moloney, and J. G. Mclnerney, "Dynamics of a semiconductor laser with optical feedback," *Phys. Rev. A,* vol. 60, pp. 1534-1537, 1999.

[18] A. Argyris, M. Boumpos, A. Bogris, and D. Syvridis,"Statistical properties of broadband chaotic signals for ultrafast true random bit sequence generation," *European Conference and Exhibition on Optical Communications(IET, 2013),* pp. 1038-1040.

[19] N. Li, B. Kim, A. Locquet, D. Choi, W. Pan, and D. S. Citrin, "Statistics of the optical intensity of a chaotic external-cavity DFB laser," *Opt. Lett.,* vol. 39, pp. 5949-5952, 2014.

[20] J. Sacher, W. Elsässer, and E. O. Göbel, "Intermittency in the coherence collaspe of a semiconductor laser with external feedback," *Phys. Rev. Lett.,* vol. 63, pp. 2224-2227, 1989.

[21] T. Mikami, K. Kanno, K. Aoyama, A. Uchida, T. Ikeguchi, T. Harayama, S. Sunada, K. Arai, K. Yoshimura, and P. Davis, "Estimation of entropy rate in a fast physical random-bit generator using a chaotic semiconductor laser with intrinsic noise," *Phys. Rev. E,* vol. 85, p. 016211, 2012.

[22] G. Aromataris and V. Annovazzi-Lodi, "Error analysis of a digital message impaired by optical chaos," *IEEE Photon. Technol. Lett.,* vol. 24, pp. 903-905, 2012.

[23] B. Dorizzi, B. Grammaticos, M. Le Berre, Y. Pomeau, E. Ressayre and A. Tallet, "Statistics and dimension of chaos in differential delay systems," *Phys. Rev. A,* vol. 35, pp. 328-339, 1987.

[24] C. R. S. Williams, J. C. Salevan, X. Li, R. Roy, and T. E. Murphy, "Fast physical random number generator using amplified spontaneous emission," *Opt. Express,* vol. 18, pp. 23584-23597, 2010.

[25] J. Zhang, Y. Wang, M. Liu, L. Xue, P. Li, A. Wang, and M. Zhang, "A robust random number generator based on differential comparison of chaotic signals," *Opt. Express,* vol. 20, pp. 7496-7506, 2012.

[26] V. N. Chizhevsky, "Symmetrization of single-sided or nonsymmetrical distribution: The way to enhance a generation rate of random bits from a physical source of randomness," *Phys. Rev. E,* vol. 82, p. 050101, 2010.

[27] I. Kanter, Y. Aviad, I. Reidler, E. Cohen, and M. Rosenbluh, "An optical ultrafast random bit generator," *Nat. Photonics,* vol. 4, pp. 58-61, 2010.
[28] L. Zunino, O. A. Rosso, and M. C. Soriano, "Characterizing the hyperchaotic dynamics of a semiconductor laser subject to optical feedback via permutation entropy," *IEEE J. Sel. Top. Quantum Electron.,* vol. 17, pp. 1250-1257, 2011.
[29] R. Lang and K. Kobayashi, "External optical feedback effects on semiconductor injection laser properties," *IEEE J. Quantum Electron.,* vol. 16, pp. 347-355, 1980.
[30] D. Rontani, A. Locquet, M. Sciamanna, D. S. Citrin, and S. Ortin, "Time-delay identification in a chaotic semiconductor laser with optical feedback: A dynamical point of view," *IEEE J. Quantum Electron.,* vol. 45, pp. 879-891, 2009.
[31] N . Li, W. Pan, L. Yan, B. Luo, X. Zou, and S. Xiang, "Enhanced two-channel optical chaotic communication using isochronous synchronization," *IEEE J. Sel. Top. Quantum Electron.,* vol. 19, p. 0600109, 2013.
[32] C. Masoller and N. B. Abraham, "Stability and dynamical properties of the coexisting attractorsof an external-cavigy semiconductor laer," *Phys. Rev. A,* vol. 57, pp. 1313-1322, 1998.
[33] J. A. Reinoso, J. Zamora-Munt, C. Masoller, "Extreme intensity pulses in a semiconductor laser with a short external cavity," *Phys. Rev. E,* vol. 87, p. 062913, 2013.

Nianqiang Li received the B.S. degree from Southwest Jiaotong University, Chengdu, China, in 2008, where he is currently pursuing Ph.D. degree. He was a visiting ph.D. student with the Prof. D. S. Citrin's Research Group, Georgia Institute of Technology, Atlanta, GA, USA, from 2013 to 2014. His current research interests include chaotic time series analysis, nonlinear dynamics in time-delayed systems, and chaos-based communications using semiconductor lasers.

Wei Pan received the Ph.D. degree from Southwest Jiaotong University, Chengdu, China, in 1999. He is currently a Professor and the Dean of the School of Information Science and Technology, Southwest Jiaotong University. He has authored or co-authored more than 100 research papers. His current research interests include semiconductor lasers, nonlinear dynamic systems, and optical communication. He is a member of the Optical Society of America and the Chinese Optical Society.

Alexandre Locquet (M'99) received the M.S. degree in electrical engineering from Facult Polytechnique de Mons, Belgium, in 2000, the Ph.D. degree in engineering science from Universit de Franche-Comt, France, in 2004, and the Ph.D. degree in electrical and computer engineering from the Georgia Institute of Technology (Georgia Tech), Atlanta, in 2005. His doctoral work was related to optical chaos-based communications. He is currently a Researcher with the Unit Mixte Internationale Georgia Tech-CNRS Laboratory, Georgia Tech Lorraine, Metz, France, and an Adjunct Professor with the School of Electrical and Computer Engineering, Georgia Tech. His interests are in semiconductor laser dynamics and chaos, nonlinear time series analysis, physical-layer security, and terahertz imaging. He has authored or co-authored over 40 journal publications and conference presentations, and one book chapter. He is a member of Eta Kappa Nu and the CNRS Dynamique et Contrôle des Ensembles Complexes research group.

V. N. Chizhevsky received the Ph.D. degree from Institute of Physics of National Academy of Sciences of Belarus, Minsk, Belarus in 1992. He is currently a Leading researcher at the same institute. He has authored or co-authored more than 50 research papers. His current research interests include nonlinear dynamics and stochastic processes in lasers, and random number generation.

David S. Citrin (M'93−SM'03) received the B.A. degree is in physics from Williams College, Williamstown, MA, in 1985, and the M.S. and Ph.D. degrees in physics from the University of Illinois at Urbana-Champaign, Urbana, in 1987 and 1991, respectively, where he worked on the optical properties of quantum wires. After receiving the Ph.D. degree, he was a Postdoctoral Research Fellow with the Max Planck Institute for Solid State Research, Stuttgart, Germany (1992−1993), where he worked on exciton radiative decay in low-dimensional semiconductor structures. From 1993 to 1995, he was a Center Fellow with the Center for Ultrafast Optical Science at the University of Michigan, Ann Arbor, where his work addressed ultrafast phenomena in quantum wells. He was an Assistant Professor of Physics with Washington State University from 1995 to 2001, at which time he joined the faculty at the Georgia Institute of Technology, Atlanta, where he is currently a Professor in the School of Electrical and Computer Engineering. His interests are in nonlinear dynamics, nano photonics, and terahertz technology. He has served as an Associate Editor for the IEEE JOURNAL OF QUANTUM ELECTRONICS. He was a recipient of the Presidential Early Career Award for Scientists and Engineers and the Friedrich Bessel Prize from the Alexander von Humboldt Stiftung.